

Stabilization of liquified-inert-gas jets for laser–plasma generation

B. A. M. Hansson,^{a)} M. Berglund, O. Hemberg, and H. M. Hertz

Biomedical and X-ray Physics, Royal Institute of Technology/SCFAB, SE-106 91 Stockholm, Sweden

(Received 18 August 2003; accepted 26 January 2004)

We investigate the hydrodynamic properties of liquified-inert-gas jets in a vacuum with a special emphasis on their stability. Such jets have applications as targets for laser–plasma generation of soft-x-ray and extreme-ultraviolet (EUV) radiation. An important example is the liquid-xenon-jet laser-plasma source, one of the source candidates for EUV lithography. A simple hydrodynamic model is not sufficient to explain experimental observations of jet stability. Evaporation-induced cooling explains observed in-flight freezing of the jet and may be a key factor influencing jet stability. It is shown how the jet stability, and, thus, the stability of the laser–plasma x-ray and EUV emission, are improved by applying localized heating to the tip of the jet-generating nozzle. © 2004 American Institute of Physics. [DOI: 10.1063/1.1687037]

I. INTRODUCTION

Laser plasmas based on inert-gas targets are attractive as negligible-debris extreme-ultraviolet (EUV) and soft-x-ray sources. An important example is the xenon-liquid-jet laser plasma,^{1,2} a potential source for EUV lithography. In this article, we investigate the stability and the hydrodynamics of such liquified-inert-gas jets in a vacuum. We specifically show how previously reported directional jet instabilities^{2–4} are improved by heating the tip of the tapered nozzle used to generate the jet.

Laser plasmas, in general, are potentially suitable as table-top sources of soft-x-ray and EUV radiation for applications, such as EUV lithography,⁵ proximity x-ray lithography,^{6–8} x-ray microscopy,⁹ and x-ray photoelectron spectroscopy.¹⁰ Attractive features of laser plasmas are high brightness, high spatial stability, and high repetition rate. However, with conventional bulk or tape targets, the operating time is limited, especially when high-repetition-rate lasers are used, since fresh target material cannot be continuously supplied for extended periods. Furthermore, conventional targets produce debris¹¹ which may destroy or coat, e.g., EUV multilayer optics or x-ray masks that are positioned close to the plasma. The amount of debris produced can be limited by replacing conventional solid targets with, e.g., gas,¹² gas-cluster,^{13,14} liquid spray,^{15,16} liquid-droplet,¹⁷ or liquid-jet^{18,19} targets. A further way to specifically eliminate the coating problem is to use a target consisting of inert atoms,²⁰ for example, noble gases like xenon, so that the evaporated target will not condense on sensitive components at room temperature. The liquified-inert-gas-jet laser–plasma source combines the advantages of being a long-operating time, low-debris target type, and using a noncontaminating target material.

The liquid-xenon-jet laser–plasma source of EUV radiation^{1,2} is of particular interest as it is one of the source candidates for EUV lithography.²¹ Lately, it has been reported that the liquid-xenon-jet laser-plasma technology is

evaluated at several further locations.^{22–24} The key advantages of this technology for EUV lithography have been described in previous publications^{25,26} and include the possibility to operate a stable plasma far from the nozzle, thereby limiting the thermal load on the nozzle at high-power operation. However, such stable laser–plasma generation requires a spatially stable liquid jet. The advantage of increasing the operating distance is one of the main motivations for studying the jet stability.

In this article, we first describe the experimental arrangement and give some background to the generation of liquified-inert-gas jets in a vacuum. Further, we report on the difficulty to sufficiently explain the stability behavior of liquified-inert-gas jets by a simple hydrodynamic theory and finally how local heating of the nozzle tip is found to increase the spatial stability of the jets drastically. We specifically report the effect on liquid-xenon jets, although the effect has also been observed for krypton.

II. EXPERIMENTAL ARRANGEMENT

The experimental arrangement for laser–plasma generation utilizing a liquified-inert-gas jet as target is shown in Fig. 1. The jet is formed by forcing gas, typically under 10–50 bar pressure, into a small reservoir cooled by a cold head to temperatures where the specific gas condenses. For Xe, this is typically 170–190 K. A tapered glass capillary nozzle with an orifice of approximately 10 μm in diameter is attached to the reservoir, producing a microscopic jet of liquified gas into a vacuum chamber. The vacuum is maintained with a turbodrag pump, typically keeping the chamber pressure at 10^{-4} – 10^{-3} mbar during operation.

Once the jet is injected into the vacuum chamber, the plasma is generated by a Nd:YAG laser typically delivering nanosecond pulses with several tens of mJ per pulse. The laser beam is focused onto the jet, achieving power densities in the 10^{11} – 10^{12} W/cm² range. The laser–plasma x-ray emission is monitored by an x-ray sensitive diode covered with an aluminum/silver absorption filter, about 300 nm thick, to remove nonsoft-x-ray radiation.

^{a)}Electronic mail: bjorn.hansson@biox.kth.se

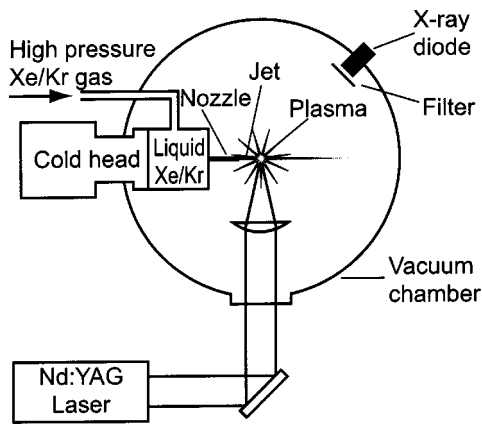


FIG. 1. The basic arrangement for liquified-inert-gas-jet laser-plasma experiments.

III. JET GENERATION AND IN-FLIGHT FREEZING

Normally, a liquid jet will spontaneously break up into droplets.²⁷ However, highly evaporating liquids, such as liquified gases, may freeze due to evaporation-induced cooling before traveling the droplet formation distance, thereby inhibiting drop formation. Whether or not droplets will form is, therefore, a question of the speed of the droplet formation process vs the jet cooling process.

The general theory for the droplet formation distance, L , is that of Weber,^{28,29}

$$L = \left(\ln \frac{d}{2\delta_0} \right) \nu \left[\left(\frac{\rho d^3}{\sigma} \right)^{0.5} + \frac{3\eta d}{\sigma} \right], \quad (1)$$

where the parameters are defined in Table I. Unfortunately, a quantitative determination of L is difficult since the initial disturbance, $\ln(d/2\delta_0)$ cannot be calculated *a priori* and it has been reported³⁰ in the range of ~ 1 – 20 . In order to estimate this term for the nozzles used in the present experiments, the droplet-breakup distance for ethanol was measured with identical nozzles and compared with the theoretical expression. Since the main question is whether or not droplets can be formed before the jet freezes, the droplet formation was stimulated by a piezoelectric crystal in order to get a lower limit to the distance. The measurement yielded a lower limit of ~ 3.5 for the constant, resulting in the following equation for the droplet-formation distance of the specific type of nozzle,

TABLE I. Important parameters for the jet stability. The values for xenon at 180 K and 30 bar are given as examples when applicable.

Parameter	Symbol	Value
Density	ρ [kg/m ³]	2854 ^a
Viscosity	η [10 ⁻³ · Pa s]	0.409 ^b
Surface tension	σ [10 ⁻³ · N/m]	15.7 ^c
Velocity of jet	ν [m/s]	40.0 ^d
Jet diameter	d [μm]	10

^aReference 40.

^bReference 41.

^cReference 42.

^dCalculated according to Ref. 31.

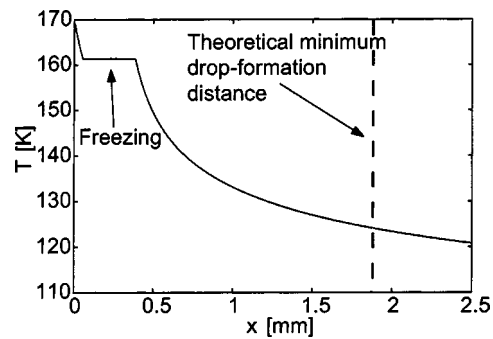


FIG. 2. The calculated cooling process of a 10 μm xenon jet injected into a vacuum at 30 bar corresponding to ~ 40 m/s. The theoretical model indicates that the jet freezes well before the droplet formation point, thereby inhibiting the formation of droplets.

$$L > 3.5\nu \left[\left(\frac{\rho d^3}{\sigma} \right)^{0.5} + \frac{3\eta d}{\sigma} \right]. \quad (2)$$

The evaporative cooling and freezing of the jet may be modeled using elementary thermodynamic arguments. Assuming xenon with an initial temperature of 170 K and an injection pressure of 30 bar, the calculated cooling/freezing process as a function of distance from the nozzle orifice is illustrated in Fig. 2. The model is described in Appendix A. In addition, the minimum droplet-formation distance according to Eq. (2) is inserted in Fig. 2. As can be seen, the jet will rapidly freeze, thereby inhibiting droplet formation. The jet velocity is calculated from the injection pressure according to Ref. 31.

Although the cooling/freezing calculation contain some uncertainties as discussed in Appendix A, it is still clear that the model predicts that the jet freezes well before the droplet formation point. This is supported by experimental evidence shown in Fig. 3. Here, the xenon jet is photographed several centimeters from the nozzle orifice. The image is taken through a microscope and using a ~ 10 ns laser pulse for illumination. At this distance, the jet is broken at several locations but no sign of general droplet formation is visible. This behavior is only possible if the jet is in solid state.

It should be mentioned that droplets of liquified gases can be generated if the jet is injected into an environment where the pressure is closer to the vapor pressure of the liquid at the temperature of the jet and, therefore, the effective evaporation rate is lower. This was first shown for oxygen and argon.³² However, the required ambient pressure is much too high for laser-plasma soft-x-ray and EUV generation purposes since the emitted radiation will rapidly be absorbed in the surrounding gas. Xenon droplets have also been generated using drop-on-demand technology,³³ but also in this case at too high ambient pressure for soft-x-ray and EUV purposes. Droplets may be produced in a high-vacuum



FIG. 3. A 10 ns-flash photograph of a xenon jet several centimeters from the nozzle orifice. The jet is broken at several locations but no signs of general droplet formation are visible.

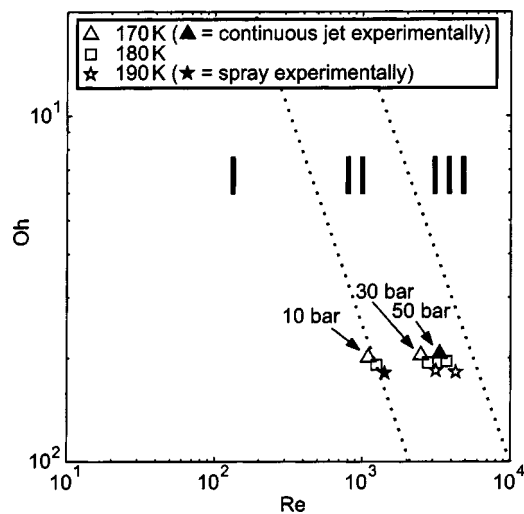


FIG. 4. Different regions of stability of a liquid jet based on the conventional theory. In region I, the jet should break up into regularly sized droplets, in region II, into droplets of many sizes, and in region III the jet should form a spray. The calculated data points are for a 10 μm diameter xenon jet.

environment using a differential pumping scheme, where the drops are formed in a chamber with higher pressure and then injected into a high vacuum.^{32,34} However, with such a scheme, it is difficult to achieve acceptable spatial stability so that the drops can be accurately hit by the laser pulses since the drop flight path is perturbed during injection³⁵ into a high vacuum.

IV. JET STABILITY

For the operation of a jet of liquified gas in a vacuum, we have identified two different stability issues. The first issue is the conventional problem that the flow from a nozzle sometimes forms a continuous jet and sometimes breaks up into a spray directly at the orifice or further downstream. The second issue is that a directional instability can be present although a continuous jet is formed. We will start by discussing the first issue.

We have found that, in order to avoid spraying, a jet of liquified gas must be operated at a temperature approaching the solidification temperature. The reason for this is, however, not sufficiently explained by the conventional theory²⁹ where the jet stability is characterized by Ohnesorge's number, $Oh = \eta / \sqrt{\delta \sigma d}$, and Reynolds' number, $Re = dV\delta/\eta$, (see Table I for data and explanation of symbols).

The conventional diagram of Fig. 4 illustrates how different values of Ohnesorge's and Reynolds' numbers should lead to different break-up phenomena of the jet.²⁹ In region I, the jet should break up into regularly sized droplets, in region II, into droplets of many sizes, and in region III, the jet should form a spray. The data points are calculated for a xenon jet of 10 μm diameter and with values for ρ , η and σ from Table I and its references. As can be seen in Fig. 4, an increase in pressure, i.e., jet velocity, should have a larger effect on the spraying behavior than a rise in temperature. However, this is not supported by experiment since a continuous jet is normally nicely operated at 50 bar and 170 K but not at 10 bar and 190 K (cf. Fig. 4). The instabilities of

regions II and III in Fig. 4 are conventionally believed to be due to the aerodynamic influence of the ambient gas. The departure in our case from the general explanation may be due to the fact that we inject our jet into a vacuum where no atmosphere will interact with the jet. In the absence of the atmospheric effects, the question of spray or continuous behavior should depend solely upon whether the jet is turbulent or not when leaving the nozzle. This is normally determined only by the Reynolds number and the nozzle geometry: turbulence increases with increasing Reynolds' number at a fixed nozzle diameter. However, turbulence alone does not fully explain the observations either since, experimentally, it is found that a 50 bar 170 K jet is more stable than a 10 bar 190 K jet even though the Reynolds number is larger for the former, as illustrated in Fig. 4. Possible explanations are that, in the high-temperature case, the initial rapid evaporation rate could produce a local atmosphere promoting instabilities or that the evaporation could induce an initial disturbance to the jet leading to spray formation. The initial evaporation rate of xenon is $2.5\times$ higher at 190 K compared to 170 K according to Eq. (A1) of Appendix A and the vapor pressure of liquid xenon: 3.5 bar at 190 K and 1.3 bar at 170 K.³⁶ The actual local gas pressure at the surface of the jet is, however, difficult to determine due to the nonequilibrium situation. Although the reason for the spraying behavior at higher temperatures is not fully understood, it will be shown below that this phenomena places limitations on how to apply nozzle heating to deal with the second type of instability, the directional instability.

Even though a continuous jet is formed at sufficiently low temperatures, a directional instability that can be as large as 1° corresponding to several jet diameters at the point of plasma formation, is often present. The occurrence frequency of this directional change is typically less than 10 Hz. Such an instability has been reported previously²⁻⁴ and makes stable plasma generation at practical distances from the nozzle difficult. Our hypothesis for the phenomena is that some substance, most probably the liquified gas itself, freeze in or around the nozzle orifice, changing the flow characteristics at the orifice. One can assume that the heavy evaporation of the jet cools the nozzle to temperatures below the freezing point of the used liquified gas. The cooling process could either be due to the evaporation of the liquid that wets the edges of the orifice or a temperature transfer from the jet that in its turn is cooled by evaporation. Nozzle cooling has actually previously been observed for normal liquids.³⁷ In order to avoid this presumed freezing, we investigated the effect of heating the nozzle tip by applying resistive heating at the tip with a thin wire. It was found that a localized heating of the tip results in stable jet formation. This phenomena was observed both for xenon and krypton. When increasing the heating power of the wire, the jet goes through a characteristic behavior where it will spray increasingly until a sudden transition at some temperature where a continuous stable jet is formed. This is illustrated in Figs. 5(a)–5(c). The tendency to spray, when heating is applied, is consistent with the observation reported above, that the jet will spray when the liquid is too warm. The sudden transition may be due to the nozzle tip warming sufficiently such that frozen

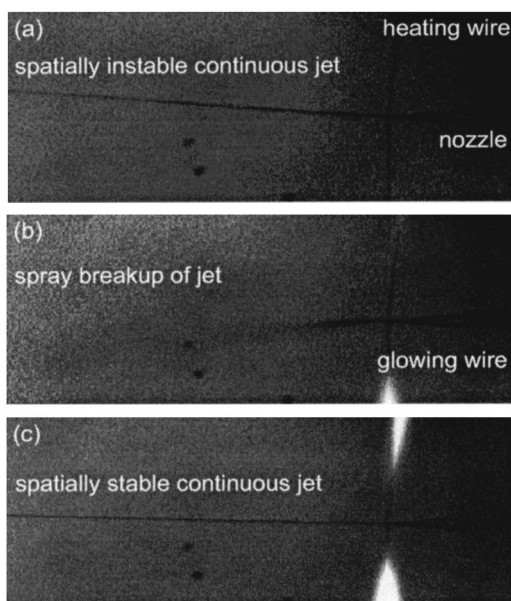


FIG. 5. Consecutive images of a 10 μm liquid-xenon jet leaving a tapered glass capillary nozzle with a thin resistive wire wound around the tip at different states of heating. With no heating (a) a spatially unstable continuous jet is formed. With some heating applied (b) the jet disintegrates to a spray but when more heating is applied the jet undergoes a sudden transition and becomes spatially stable (c).

material is abruptly released, creating a smoother nozzle exit. This smoother exit will result in less initial disturbance to the jet, so that stable operation is possible although the jet is heated somewhat. It should be noted, though, that we have not been able to actually observe frozen material leaving the nozzle, so the explanation is still a hypothesis. However, the observation of a sudden transition strongly supports our explanation. If the heating is increased further, the jet will start spraying again, which also is in accordance with the discussion about how the jet sprays at higher temperatures.

We have also observed that, while applying nozzle–tip heating, the jet must be operated at some minimum pressure to achieve a continuous jet. If the injection pressure is too low, a sudden transition is still observed with increased heating, but this is only a transition between two modes of spraying. One explanation for this is that the liquid must pass the hot wire with sufficient velocity so as to avoid bulk heating. Although the actual temperature increase would be difficult to estimate, one can assume that it is inversely proportional to the speed with which the jet passes the heated nozzle region. If the nozzle pressure is too low, the jet moves so slowly past the heated nozzle that the jet reaches a temperature that leads to spraying even for a smooth nozzle exit. In the same way, the heating must be applied very locally around the tip in order to generate a continuous stable stream. If the heating is not applied close enough to the tip, too much power is needed to heat the actual tip so that the liquid will be heated to a spraying temperature before the directional instabilities disappear.

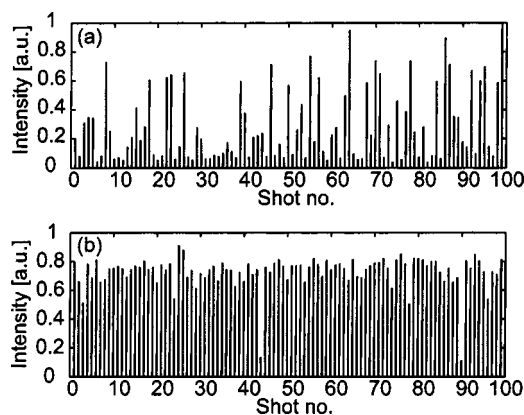


FIG. 6. The improved emission stability (previously published in Ref. 38) that was the result of applying nozzle heating. The relative standard deviation was 89% at 2.9 mm from the nozzle without heating in (a) and 16% at 5.2 mm from the nozzle with heating in (b).

V. LASER–PLASMA SOFT-X-RAY AND EXTREME ULTRAVIOLET GENERATION BASED ON A STABILIZED LIQUID-XENON-JET TARGET

The previously published³⁸ drastic increase in emission stability from a liquid-xenon-jet laser plasma was an initial result achieved by the heating method described above. The signal from the x-ray diode was logged using a gated integrator and a computer interface. Figure 6(a) is the signal from 100 consecutive shots at 2.9 mm distance from the nozzle exit with no heating applied. The relative standard deviation is 89% in this case. Figure 6(b), on the other hand, is from 100 consecutive shots at 5.2 mm from the nozzle exit with heating applied. Although the distance from the nozzle exit to the plasma is increased, the relative standard deviation is improved drastically to 16%. In both cases, the relative standard deviation of the laser pulse energy is below 3%. It should be noted that the nature of the filter in front of the x-ray diode is such that x rays in the $\lambda=1\text{--}2$ nm range are predominantly detected instead of the 10–15 nm wavelength range of interest for EUV lithography. The early measurements demonstrate that plasma generation, in general, is significantly more stable when heating is applied.

VI. SUMMARY

The stability of liquified-inert-gas jets in a vacuum has been studied in order to understand previously reported stability problems limiting their applicability as targets, specifically in laser–plasma EUV sources for lithography. It is found that previously reported directional instabilities of otherwise spatially continuous jets can be remedied by applying local heating at the nozzle orifice. Most likely, this heating is effective since the heavy evaporation of the liquified-inert-gas jets in a vacuum otherwise will cool the nozzle tip so that some substance, most probably the liquified gas itself, freezes in the tip, thereby changing the flow characteristics of the jet. It was also found that the transition from a spatially continuous jet to spraying behavior is not sufficiently described by a simple hydrodynamic theory. Specifically, a stronger influence of jet temperature than jet speed was ob-

TABLE II. Explanation of symbols used in the evaporation and cooling calculation.

Symbol	Significance
$C_{P(\ell)}$	Specific heat of liquid. ^a
$C_{P(s)}(T)$	Specific heat of solid. ^b
k	Boltzmann's constant.
L_f	Latent heat of fusion. ^c
L_v	Latent heat of vaporization. ^c
m	Atomic mass.
$P(T)$	Saturated vapor pressure of liquid ^d or solid ^b xenon.
r	Jet radius.
T	Temperature.
T_f	Temperature at freezing point
α	Sticking coefficient. ^e
$\phi(T)$	Outward molecular flux.
ρ_s	Density of solid xenon, as sumed to be constant with temperature. ^b
$\rho_\ell(T)$	Density of saturated liquid xenon. ^a

^aReference 40.^bReference 41.^cReference 43.^dReference 36.^eReferences 44–46.

served contrary to theory. The initial evaporation of the jet during injection into a vacuum may be the source of this discrepancy with theory.

APPENDIX A: EVAPORATION AND COOLING OF A LIQUIFIED-INERT-GAS JET

When the liquified-inert-gas jet is injected into a vacuum, the heavy evaporation will quickly cool the jet leading to rapid freezing. In this appendix, we model the temperature of the jet as a function of time by an analysis similar to that earlier performed for liquid hydrogen.³⁹ The symbols used in the calculation are given in Table II. In the calculation, the jet radius is assumed to be constant although this is obviously not true for the real case. It is also assumed that the jet is in a total vacuum, although a local gas atmosphere, might be present in the close vicinity of the jet due to its evaporation. The effect of such a local gas cloud is not included in the following model.

The emitted molecular flux from the jet at a specific jet temperature is equal to the number of molecules striking a surface at equilibrium vapor pressure at that temperature with the addition of the sticking coefficient, i.e., the probability that a molecule hitting the surface does not bounce. Thus, the emitted flux is

$$\phi(T) = \alpha \frac{1}{4} P(T) \sqrt{\frac{8}{\pi k T m}}. \quad (\text{A1})$$

The mass loss over a small time, δt , in a segment of the liquid jet due to this evaporation can be expressed as

$$\frac{\delta M}{M} = - \frac{\phi(T) m \pi 2 r}{\pi r^2 \rho_\ell(T)} \delta t. \quad (\text{A2})$$

At the same time, the mass loss associated with a reduction of temperature is

$$\frac{\delta M}{M} = \frac{C_{P(\ell)}}{L_v} \delta T. \quad (\text{A3})$$

Equations (A2) and (A3) can be combined to

$$\frac{\delta T}{\delta t} = -2 \frac{L_v \phi(T) m}{C_{P(\ell)} r \rho_\ell(T)}, \quad (\text{A4})$$

resulting in an expression for the temperature as a function of time.

At the freezing point, the evaporation leads to a phase transition rather than a decrease in temperature. The fraction $\Delta M/M$ of the jet that will evaporate is determined by the relation

$$\frac{\Delta M}{M} = \frac{L_f}{L_f + L_v}, \quad (\text{A5})$$

and the time it takes for this fraction to evaporate and the jet to freeze is

$$t_f = \frac{\Delta M}{M} \frac{\pi r^2 \rho_\ell(T_f)}{m \phi(T_f) 2 \pi r}. \quad (\text{A6})$$

Finally, further cooling of the frozen jet is given by

$$\frac{\delta T}{\delta t} = -2 \frac{(L_v + L_f) \phi(T) m}{C_{P(s)}(T) r \rho_s(T)}. \quad (\text{A7})$$

If Eqs. (A4), (A6), and (A7) are combined and numerically integrated, the temperature of the jet as a function of time after injection is found. The temperature of a 10 μm xenon jet as a function of the distance from the nozzle orifice is plotted in Fig. 2. The data were obtained assuming an initial xenon temperature of 170 K and a driving pressure of 30 bar, resulting in a jet velocity of ~ 40 m/s calculated according to Ref. 31.

¹L. Rymell, M. Berglund, B. A. M. Hansson, and H. M. Hertz, *Proc. SPIE* **3676**, 421 (1999).

²B. A. M. Hansson, L. Rymell, M. Berglund, and H. M. Hertz, *Microelectron. Eng.* **53**, 667 (2000).

³M. Berglund, L. Rymell, H. M. Hertz, and T. Wilhein, *Rev. Sci. Instrum.* **69**, 2361 (1998).

⁴M. Wieland, M.S. thesis, Institut für Röntgenphysik der Georg-August-Universität Göttingen, 1999.

⁵D. A. Tichenor, G. D. Kubiak, M. E. Malinowski, R. H. Stulen, S. J. Haney, K. W. Berger, L. A. Brown, R. R. Freeman, W. M. Mansfield, O. R. Wood II *et al.*, *Opt. Lett.* **16**, 1557 (1991).

⁶D. J. Nagel, R. R. Whitlock, J. R. Grieg, R. E. Pechacek, and P. M. C. , *Proc. SPIE* **135**, 46 (1978).

⁷L. Malmqvist, A. L. Bogdanov, L. Montelius, and H. Hertz, *J. Vac. Sci. Technol. B* **15**, 814 (1997).

⁸C. J. Gaeta, H. Rieger, I. C. E. Turcu, R. A. Forber, K. L. Cassidy, S. M. Campeau, M. F. Powers, J. R. Maldonado, J. H. Morris, R. M. Foster *et al.*, *Proc. SPIE* **4688**, 818 (2002).

⁹M. Berglund, L. Rymell, M. Peuker, T. Wilhein, and H. M. Hertz, *J. Microsc.* **197**, 268 (2000).

¹⁰H. Kondo, T. Tomie, and H. Shimizu, *Appl. Phys. Lett.* **69**, 182 (1996).

¹¹R. Bobkowski and R. Fedosejevs, *J. Vac. Sci. Technol. B* **14**, 1973 (1996).

¹²H. Fiedorowicz, A. Bartnik, P. Parys, and Z. Patron, in *X-ray optics and microanalysis 1992*, edited by P. B. Kenway, Institute of Physics Conference Series, Vol. 130 (IOP, Bristol, 1993), pp. 515–518.

¹³H. Fiedorowicz, A. Bartnik, Z. Patron, and P. Parys, *Laser Part. Beams* **12**, 471 (1994).

¹⁴G. D. Kubiak, L. J. Bernardez, K. D. Krenz, D. J. O'Connell, R. Gu-

- towski, and A. M. M. Todd, OSA Trends Opt. Photonics Ser. **4**, 66 (1996).
- ¹⁵R. H. Moyer, H. Shields, A. Martos, S. W. Fornaca, R. J. St. Pierre, and M. B. Petach, Proc. SPIE **4343**, 249 (2001).
- ¹⁶M. Segers, M. Bougeard, E. Caprin, T. Ceccotti, D. Normand, M. Schmidt, and O. Sublemontier, Microelectron. Eng. **61**, 139 (2002).
- ¹⁷L. Rymell and H. M. Hertz, Opt. Commun. **103**, 105 (1993).
- ¹⁸H. M. Hertz, L. Malmqvist, L. Rymell, and M. Berglund, US Patent No. 6,002,744 (1999).
- ¹⁹L. Malmqvist, L. Rymell, M. Berglund, and H. M. Hertz, Rev. Sci. Instrum. **67**, 4150 (1996).
- ²⁰T. Mochizuki and C. Yamanaka, Proc. SPIE **733**, 23 (1987).
- ²¹J. E. Bjorkholm, Intel Tech. J. **Q3**, 1 (1998).
- ²²H. Shields, S. W. Fornaca, M. B. Petach, M. Michaelian, R. D. McGregor, R. H. Moyer, and R. J. St. Pierre, Proc. SPIE **4688**, 94 (2002).
- ²³U. Stamm, I. Ahmad, V. M. Borisov, F. Flohrer, K. Gaebel, S. Goetze, A. S. Ivanov, O. B. Khristoforov, D. Kloepfel, P. Koehler *et al.*, Proc. SPIE **4688**, 122 (2002).
- ²⁴A. Endo, H. Sato, H. Komori, T. Abe, H. Mizoguchi, K. Toyoda, and Y. Horiike, *Proceedings of the EUVL Source Workshop* (Sematech, Austin, 2003), <http://www.semtech.org>.
- ²⁵B. A. M. Hansson, L. Rymell, M. Berglund, O. Hemberg, E. Janin, J. Thoresen, and H. M. Hertz, Proc. SPIE **4506**, 1 (2001).
- ²⁶B. A. M. Hansson, R. Lars, M. Berglund, O. E. Hemberg, E. Janin, J. Thoresen, S. Mosesson, J. Wallin, and H. M. Hertz, Proc. SPIE **4688**, 102 (2002).
- ²⁷L. Rayleigh, Proc. London Math. Soc. **10**, 4 (1879).
- ²⁸C. Weber, Ztschr. F. Angew. Math. Mech. **11**, 136 (1931).
- ²⁹A. H. Lefebvre, *Atomization and Sprays*, Combustion: An international series (Hemisphere, New York, 1989).
- ³⁰R. E. Phinney, AIChE J. **18**, 432 (1972).
- ³¹O. Hemberg, B. A. M. Hansson, and H. M. Hertz, Proc. SPIE **4144**, 38 (2000).
- ³²M. Tanimoto, *Proceedings of the 7th Symposium on Fusion Technology* (Pergamon Press, Oxford, 1972), pp. 267–272.
- ³³M. J. Gouge and P. W. Fisher, Rev. Sci. Instrum. **68**, 2158 (1997).
- ³⁴C. Foster, K. Kim, R. J. Turnbull, and C. D. Hendricks, Rev. Sci. Instrum. **48**, 625 (1977).
- ³⁵B. Trostell, Nucl. Instrum. Methods Phys. Res. A **362**, 41 (1995).
- ³⁶J. Lielmezs, K. G. Astley, and J. A. McEvoy, Termochim. Acta **52**, 9 (1982).
- ³⁷O. Hemberg, B. A. M. Hansson, M. Berglund, and H. M. Hertz, J. Appl. Phys. **88**, 5421 (2000).
- ³⁸B. A. M. Hansson, M. Berglund, O. Hemberg, and H. M. Hertz, *Proceedings of the Second Annual International Workshop on EUV Lithography* (Sematech, Austin, 2000), <http://www.semtech.org>.
- ³⁹I. J. Spalding, Energia Nucleare **21**, 176 (1974), and references therein.
- ⁴⁰R. T. Jacobsen, S. G. Penoncello, and E. W. Lemmon, *Thermodynamic Properties of Cryogenic Fluids*, International cryogenics monograph series (Plenum, New York, 1997).
- ⁴¹V. A. Rabinovic, *Thermophysical Properties of Neon, Argon, Krypton, and Xenon*, National Standard Data Service of the USSR. a series of property tables (Hemisphere Springer, Berlin, 1987).
- ⁴²B. L. Smith, P. R. Gardner, and E. H. C. Parker, J. Chem. Phys. **47**, 1148 (1967).
- ⁴³Landolt-Börnstein, *Zahlenwerte und Funktionen...* (Springer Verlag, 1967), pp. 172–173, sechste auflage, IV Band, 4. Teil.
- ⁴⁴D. Dunikov (personal communication).
- ⁴⁵K. Yasuoka, Y. Matsumoto, and M. Kataoka, J. Chem. Phys. **101**, 7904 (1994).
- ⁴⁶S. I. Anisimov, D. O. Dunikov, V. V. Zhakhovskii, and S. P. Malysenko, J. Chem. Phys. **110**, 8722 (1999).